PNAS
www.pnas.org

Supplementary Information for

Early evidence for mounted horseback riding in northwest China

Yue Li, Chengrui Zhang, William Timothy Treal Taylor, Liang Chen, Rowan K. Flad, Nicole Boivin, Huan Liu, Yue You, Jianxin Wang, Meng Ren, Tongyuan Xi, Yifu Han, Rui Wen, Jian Ma

* To whom correspondence may be addressed: Jian Ma
Email: eurasiansteppes@126.com

This PDF file includes:

Supplementary Information Text

Human Pathologies at Shirenzigou

Human osteological evidence from Shirenzigou provides indirect support for the practice of horse riding. Two specific categories of abnormalities are worth mentioning. The individual (male, adult) from the burial M003 had a remarkable curved femoral diaphysis, with the height of the arc reaching 51.0mm **(Fig. S4)**. This is much higher than that of a normal human femur from M004 (37.0mm). Human femora from burials M008, M011, M013, and M015 also exhibited curved diaphysis, suggesting that this category of abnormality was not uncommon among residents at Shirenzigou. The preliminary results of an on-going research project have shown that Shirenzigou people exhibited more pronounced greater trochanters and femoral crests (i.e., linea aspera) than their counterparts in the Yellow River valley. In addition, the femur of one deceased (male, 45-50 years old) in burial M013 exhibited a noticeable facet on the femoral neck. More specifically, it extended from the articular surface of the femoral head toward the anterior aspect of the femoral neck. This facet is generally known as the Poirier's facet in the literature (1, 2).

Despite the possibility of heredity, the above-mentioned bony imprints on human femora from Shirenzigou burials may have been responses to biomechanical stress. An osseous non-metric variation of the human femur, the Poirier's facet has been considered as the result of habitual squatting or cross-legged activities associated with flexion and abduction of the thigh during normal locomotion (3-5). In more recent research on human remains from archaeological contexts, the presence of the Poirier's facet has often been associated with horse riding (2, 5-9). Strongly developed greater trochanter and linea aspera have been considered as indicative of strong adductor muscles (5). The development of adductor muscles would be common in the context of horse riding because the rider had to maintain balance on horseback to prevent falling (i.e., a gripping action), during which the adductor muscles bears much strain (7, 10, 11). In addition, the curving of the femoral diaphysis may have been the results of frequent horseback riding activities at a young age (10, 11).

Osteoarthritis data have been used to reconstruct aspects of human behavior (3, 9, 12). Osteological studies of modern jockeys have shown that horse riders tend to suffer higher incidences of degenerative alterations of cervical and lumbar vertebrae (13). It is noteworthy that some of the humans interred at Shirenzigou exhibited severe osteoarthritis or fusion on the body or articular facets of their cervical and lumbar vertebrae, which is indicative of frequent riding.

Fig. S1. The natural landscape surrounding the sites of Shirenzigou and Xigou. Photo by Chengrui Zhang.

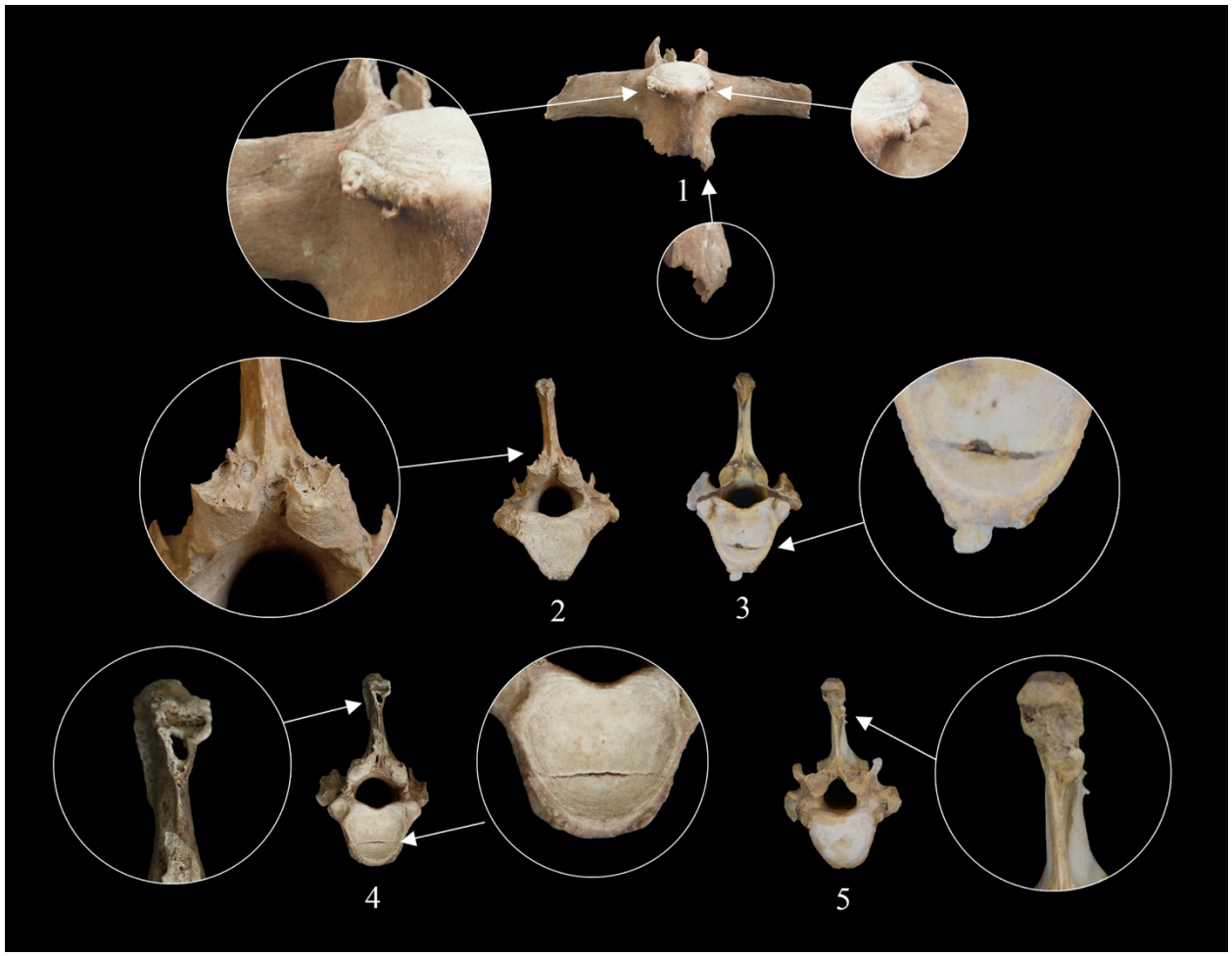

Fig. S2. Some close-ups of vertebral abnormalities on horses from Shirenzigou and Xigou. Figure by Yue Li and Yifu Han.

1. Horse 8: L1, ventral view, osteophytes (ventral part of vertebral body); 2. Horse 8: T16, caudal view, osteophytes (posterior articular process); 3. Horse 2: T13, caudal view, osteophytes and horizontal fracture (posterior articular surface of vertebral body); 4. Horse 8: T15, caudal view, horizontal fracture (posterior articular surface of vertebral body), overriding/joining of dorsal spinous processes (spinous process); 5. Horse 2: T16, cranial view, overriding/joining of dorsal spinous processes.

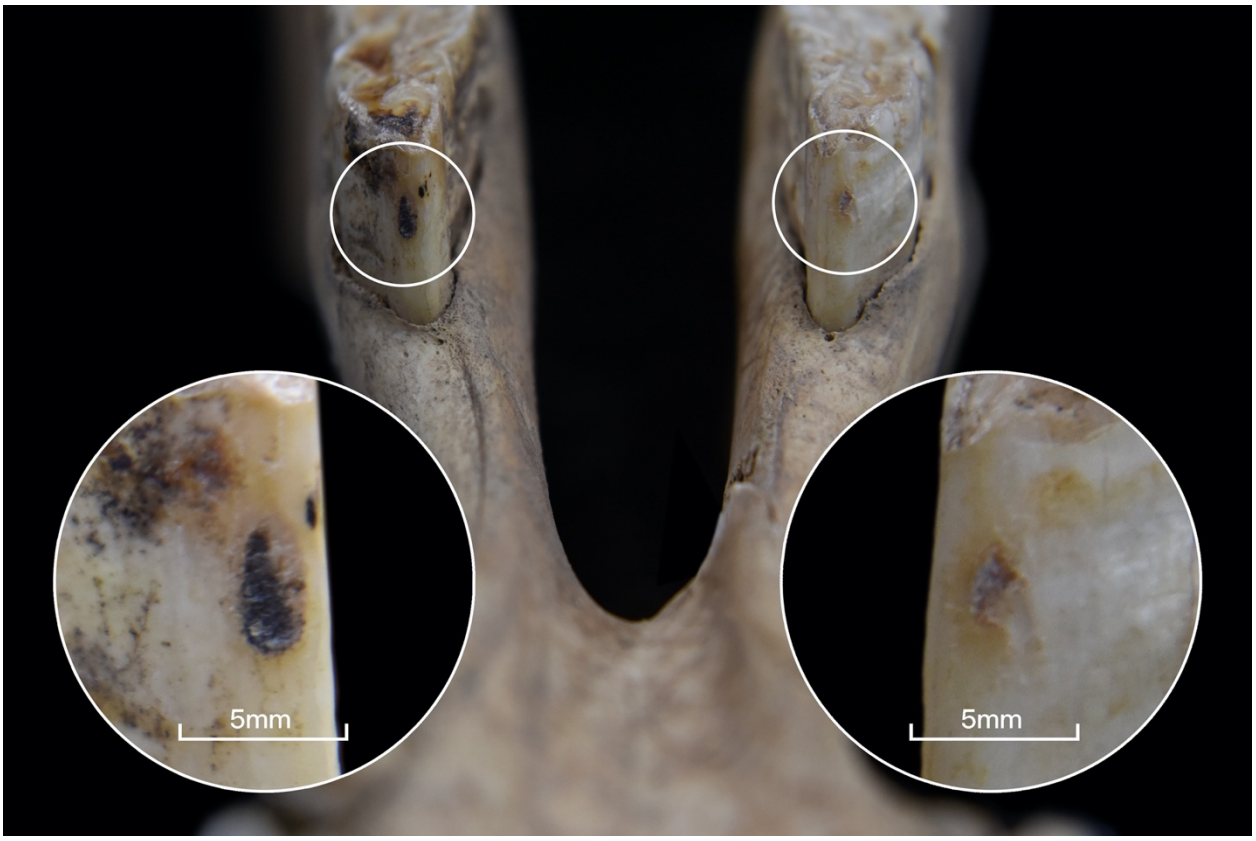

Fig. S3. The shallow chips on the anterior surface of lower second premolars of Horse 3. The chip on the right side measures 4.73mm by 2.44mm, and the left 3.54mm by 2.25mm. Figure by Yue Li and Yifu Han.

Fig. S4. Curved diaphysis exhibited on human femora from burials M011 (*Top*) and M008 (*Bottom*) at Shirenzigou. Photo by Liang Chen.

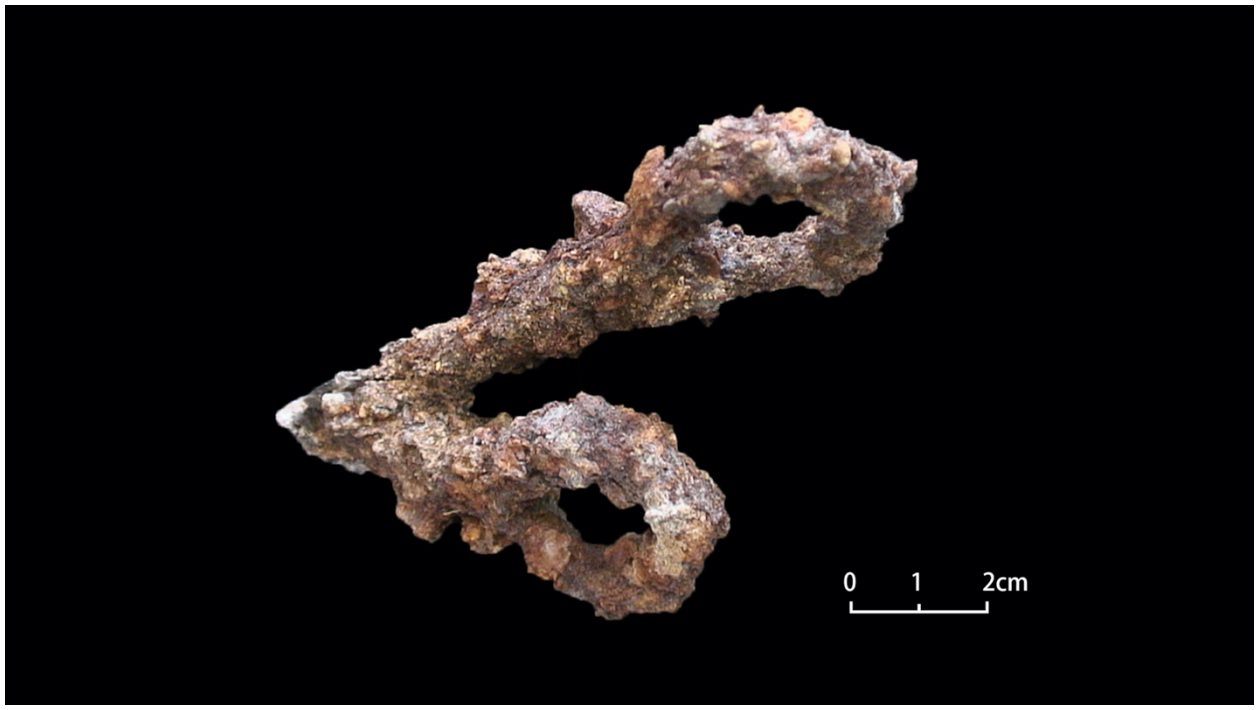

Fig. S5. The iron horse bit from burial M001 at Shirenzigou. Photo by Jian Ma.

Fig. S6. Photo showing bone arrowheads from burial M013 at Shirenzigou (*Left*). These arrowheads were either single tanged or double tanged, with an average length of 66.4mm. The two arrowheads presented here were M013:9 and M013:10 (*Right*). Photo by Jian Ma.

Table S1. Radiocarbon age determinations for horses from Shirenzigou and Xigou.

Horse ID	Site	Field Code	Material Dated	Laboratory Code	Conventional Age (BP)	Cal. BC (95.4%)
1	Shirenzigou	06BSDM001	Femur	BA-110565	2205 ± 30	370-196 (95.4%)
2	Shirenzigou	06BSDM011	Femur	BA-110567	2230 ± 25	382-344 (18.8%) 324-205 (76.6%)
3	Shirenzigou	06BSDM012	Humerus	BA-110563	2230 ± 25	382-344 (18.8%) 324-205 (76.6%)
4	Shirenzigou	07BSDM012K2	Femur	BA-110566	2150 ± 25	355-292 (29.5%) 231-97 (65.9%)
5	Shirenzigou	07BSDM012K3	Femur	BA-110564	2265 ± 30	399-350 (44.4%) 306-209 (51.0%)
7	Xigou	12XBXM1	Phalanx II	Beta-498196	2180 ± 30	361-168 (95.4%)
8	Xigou	12XBXM1K1	Phalanx II	Beta-498197	2200 ± 30	366-192 (95.4%)

Table S2. OxCal code for the Bayesian modeling.

The Bayesian modeling was conducted in OxCal v4.3.2 (14) using IntCal13 as the calibration curve (15).

1. Uniform Model

```
Plot()
 {
  Sequence("Shirenzigou and Xigou")
  {
   Boundary("Start");
   Phase("Phase")
   {
    R_Date("BA-110564  (Horse 5)", 2265, 30);
    R_Date("BA-110563  (Horse 3)", 2230, 25);
    R_Date("BA-110567  (Horse 2)", 2230, 25);
    R_Date("BA-110565  (Horse 1)", 2205, 30);
    R_Date("Beta-498197  (Horse 8)", 2200, 30);
    R_Date("Beta-498196  (Horse 7)", 2180, 30);
    R_Date("BA-110566  (Horse 4)", 2150, 25);
    Span("Span of SX dates");
    Interval("Duration SX");
    Sum("SX");
   };
   Boundary("End");
  };
 };
```

2. Trapezoid Model

```
Plot()
 {
  Sequence("Shirenzigou and Xigou")
  {
   Boundary("Start")
   {
    Transition("T");
    Start("S");
```

```
  End("E");
 };
 Phase("Phase")
 {
  R_Date("BA-110564  (Horse 5)", 2265, 30);
  R_Date("BA-110563  (Horse 3)", 2230, 25);
  R_Date("BA-110567  (Horse 2)", 2230, 25);
  R_Date("BA-110565  (Horse 1)", 2205, 30);
  R_Date("Beta-498197  (Horse 8)", 2200, 30);
  R_Date("Beta-498196  (Horse 7)", 2180, 30);
  R_Date("BA-110566  (Horse 4)", 2150, 25);
  Span("Span of SX dates");
  Interval("Duration SX");
  Sum("SX");
 };
 Boundary("End")
 {
  Transition("T");
  Start("S");
  End("E");
 };
};
```

Table S3. Distribution of vertebral abnormalities across horses examined.

(Legend: C, cervical vertebrae; T, thoracic vertebrae; L, lumbar vertebrae)

Horse ID	Osteophyte	Spinal fusion	Horizontal fracture on epiphysis	Overriding/joining of dorsal spinal processes
1	T1-T2, T12-T18; L1-L4; five unidentified vertebrae from T3-T11		T13	T12-L1
2	C7; T4, T6-T8, T12-T18; L1-L4		T13	T13-T16, T18-L4
3	T1-3, T5-T9, T12-T18; L1-L5		T13	T14-T16
4	C7; T1-T7, T10-T17; L1-L4; Sacrum	L5-L6		
5	T4-T6, T12, T14-T18; L3	L5-L6		
6	T2, T5-T11, T13-T18; L4-L6; Sacrum			T13-T18
7	C1, C5-6; T1, T3-T4, T13-T18; L1-L6; Sacrum	L2-L3, L4-L6	T14, T15, T16, T18	T13-T18; L4-L5
8	C7; T1-T7, T10, T14-T18; L1-L6			T14-T18; L1-L3

Table S4. Discernable asymmetry of vertebral abnormalities in terms of severity.

(Legend: C, cervical vertebrae; T, thoracic vertebrae; L, lumbar vertebrae; L, left side; R, right side)

	Horse 1		Horse 2		Horse 3		Horse 4		Horse 5		Horse 6		Horse 7		Horse 8	
Vertebra	L	R	L	R	L	R	L	R	L	R	L	R	L	R	L	R
C1					●									●		
C2																
C3																
C4																
C5																
C6																
C7															●	
T1	●	●			●											
T2		●			●	●	●				●	●			●	
T3					●	●		●								
T4			●			●	●	●	●							●
T5						●	●		●							●
T6					●		●									●
T7					●	●	●		●						●	
T8			●	●		●										
T9																
T10																
T11							●									
T12	●		●		●		●		●							
T13	●		●		●		●									
T14				●	●		●			●	●	●	●		●	
T15	●	●		●				●	●		●		●		●	
T16	●							●		●			●		●	●
T17	●		●					●				●				●
T18	●			●						●				●	●	
L1	●	●	●	●		●										●
L2			●												●	
L3	●				●				●							
L4			●		●		●								●	
L5						●				●					●	
L6					●					●					●	
Sacrum					●											
Number	10*	8†	9	5	13	8	10	7	6	5	3	3	4	3	11	6
%	55.6	44.4	64.3	35.7	61.9	38.1	58.8	41.2	54.5	45.4	50.0	50.0	57.1	42.9	64.7	35.3

* One vertebra, with abnormalities on the left side, from the five unidentified vertebrae of Horse 1 was counted in but not marked "●" in the table.

† Four vertebrae, with abnormalities on the right side, from the five unidentified vertebrae of Horse 1 were counted in but not marked "●" in the table.

Table S5. Measurements of grooves on nasal bones for horses in this research (Unit: mm).

(Legend: MD, medial depth; LD, lateral depth; NOS, nuchal ossification score)

Horse ID	Age	Sex	MD-Left	MD - Right	LD - Left	LD - Right	NOS
1	14-16	Likely Female	0.43	N/A	0.00	N/A	3/-
2	9	Male	N/A	0.25	N/A	0.22	2/0
3	11	Male	0.26	0.38	0.72	0.65	3/1
4	15-16	Female	0.85	N/A	0.95	N/A	4
5	9-10	Male	N/A	0.80	N/A	0.92	3/2
7	11-12	Male	1.09	0.72	N/A	0.00	5

Table S6. Data for enamel or dentine exposure and beveling of lower second premolars (Unit: mm).

(Legend: EDE, enamel or dentine exposure; EDH, height of enamel or dentine exposure; EDW, width of enamel or dentine exposure; L, left; R, right)

Horse ID	EDE-Location	EDE-Shape	EDH	EDW	Bevel	Greaves Effect	Bevels in Occlusal State
1	Front & lateral surfaces (L) Front surface (R)	- (L) Rectangle (R)	- (L) 4.09 (R)	- (L) 2.67 (R)	- (L) 3.71 (R)	No	-
2	Front surface (L) Front surface (R)	Thin strip (L) - (R)	13.86 (L) - (R)	3.29 (L) - (R)	4.66 (L) - (R)	No	No
3	Front surface (L) Front surface (R)	Wide rectangle (L) Wide rectangle (R)	15.87 (L) 15.75 (R)	4.27 (L) 4.64 (R)	5.47 (L) 3.28 (R)	No	Yes
5	Lateral surface (L) Lateral surface (R)	Narrow rectangle (L) Pointed triangle (R)	3.50 (L) 4.37 (R)	7.61 (L) 2.88 (R)	2.16 (L) 4.15 (R)	No	Yes
6	Front surface (L) - (R)	Thin strip (L) Thin strip (R)	9.72 (L) 7.15 (R)	2.14 (L) 2.5 (R)	4.14 (L) 5.07 (R)	No	-
7	Front surface (L) Front surface (R)	Thin strip (L) Thin strip (R)	11.32 (L) 13.77 (R)	3.01 (L) 3.14 (R)	No bevel (L) No bevel (R)	No	No

SI References

1. M. Finnegan, Non-metric variation of the infracranial skeleton. *J. Anat.* **125**, 23-37 (1978).
2. D. Owsley, K. Bruwelheide, R. Kardash, Recovery and analysis of Jamestown rediscovery south churchyard burials from the 1999 field season. *The Journal of the Jamestown Rediscovery Center* **1**, 1-8 (2001).
3. J. L. Angel, The reaction area of the femoral neck. *Clin. Orthop. Relat. Res.* **32**, 130-142 (1964).
4. E. Trinkaus, Squatting among the Neanderthals: A problem in the behavioral interpretation of skeletal morphology. *J. Archaeol. Sci.* **2**, 327-351 (1975).
5. T. Molleson, J. Blondiaux, Riders' bones from Kish. *Camb. Archaeol. J.* **4**, 312-316 (1994).
6. K. J. Reinhard *et al.*, "Trade, contact, and female health in northeast Nebraska" in *In the Wake of Contact: Biological Responses to Conquest*, C. S. Larse, G. J. Milner, Eds. (Wiley-Liss, New York, NY, 1994), pp. 63-74.
7. T. Molleson, A method for the study of activity related skeletal morphologies. *Bioarchaeology of the Near East* **1**, 5-33 (2007).
8. R. K. Wentz, N. T. De Grummond, Life on horseback: palaeopathology of two Scythian skeletons from Alexandropol, Ukraine. *Int. J. Osteoarchaeol.* **19**, 107-115 (2009).
9. A. Y. Khudaverdyan, H. H. Khachatrya, L. G. Eganyan, The human skeleton from the late Iron Age burial of Shirakavan (Armenia): a case study. *Bulletin of the International Association for Paleodontology* **11**, 5-61 (2017).
10. M. Schultz *et al.*, Xinjiang Yutian Xian Liushui Mudi Ershiliuhao Mu Chutu Rengu De Gubinglixue He Renleixue Chubu Yanjiu. *Kaogu* **3**, 86-91 (2008).
11. D. Wei *et al.*, Xinjiang Hami Heigouliang Mudi Chutu Rengu De Chuangshang Bingli Ji Yichang Xingtai Yanjiu. *Acta Anthropol. Sin.* **21**, 176-186 (2012).
12. C. F. Merbs, The pathology of a La Jollan skeleton from Punta Minitas, Baja, California. *PCAS Quarterly* **16**, 37-43 (1980).
13. A. Tsirikos *et al.*, Degenerative spondyloarthropathy of the cervical and lumbar spine in jockeys. *Orthopedics* **24**, 24561-24564 (2001).
14. C. Bronk Ramsey, Methods for summarizing radiocarbon datasets. *Radiocarbon* **59**, 1809-1833 (2017).
15. P. J. Reimer *et al.*, IntCal13 and marine13 radiocarbon age calibration curves 0-50,000 years cal BP. *Radiocarbon* **55**, 1869-1887 (2013).